

THE EXTREME TYPE I PLANETARY NEBULA M2-52¹

M. Peña and S. Medina

Instituto de Astronomía
Universidad Nacional Autónoma de México

Received 2001 August 14; accepted 2002 February 12

RESUMEN

Se presentan los resultados obtenidos a partir de espectroscopía de alta resolución de la parte central de la nebulosa planetaria bipolar M2-52 que muestra un tipo morfológico Br. Hemos confirmado que M2-52 es una nebulosa de Tipo I de Peimbert, con un espectro rico en líneas de alto y bajo grado de ionización y un fuerte enriquecimiento de He y N. La composición química del gas ionizado es: $\text{He}/\text{H} = 0.165 \pm 0.010$, $\text{O}/\text{H} = (2.6 \pm 0.5) \times 10^{-4}$, $\text{N}/\text{O} = 2.3 \pm 0.3$, $\text{Ne}/\text{O} = 0.37 \pm 0.10$, $\text{Ar}/\text{O} = (9.2 \pm 2.0) \times 10^{-3}$ y $\text{S}/\text{O} > 2.0 \times 10^{-3}$. La velocidad de expansión de la nebulosa es, en promedio, de $20 \pm 2 \text{ km s}^{-1}$ y varía ligeramente dependiendo del ión considerado. Los iones de menor grado de ionización, N^+ y S^+ , muestran $v_{\text{exp}} \sim 18 \text{ km s}^{-1}$, O^{++} y He^+ muestran $v_{\text{exp}} \sim 20 \text{ km s}^{-1}$, en tanto que He^{++} y H^+ muestran $v_{\text{exp}} \sim 22 \text{ km s}^{-1}$. Es posible que la zona de N^+ y S^+ esté siendo frenada por el anillo de material molecular encontrado alrededor de la estrella.

ABSTRACT

High-resolution spectrophotometric data of the central zone of the Br-type planetary nebula M2-52 are presented. The nebula has a rich spectrum, with high and low excitation lines. The chemical composition derived from the spectra shows that He and N are very enhanced in M2-52. Thus, this object can be classified as an extreme Peimbert's Type I PN. The chemical composition of the ionized gas is: $\text{He}/\text{H} = 0.165 \pm 0.010$, $\text{O}/\text{H} = (2.6 \pm 0.5) \times 10^{-4}$, $\text{N}/\text{O} = 2.3 \pm 0.3$, $\text{Ne}/\text{O} = 0.37 \pm 0.10$, $\text{Ar}/\text{O} = (9.2 \pm 2.0) \times 10^{-3}$ and $\text{S}/\text{O} > 2.0 \times 10^{-3}$. The expansion velocity of the nebula is, on average, about $20 \pm 2 \text{ km s}^{-1}$, but the low ionization species (N^+ and S^+) seem to systematically show slightly lower expansion velocities (18 km s^{-1}) than O^{++} and He^+ which have $v_{\text{exp}} = 20 \text{ km s}^{-1}$, while H^+ and He^{++} have $v_{\text{exp}} \sim 22 \text{ km s}^{-1}$. This behavior could indicate that the outer zones of the ionized gas are being decelerated by the molecular ring located around the central star.

Key Words: ISM: ABUNDANCES — ISM: KINEMATICS AND DYNAMICS — PLANETARY NEBULAE: INDIVIDUAL (M2-52)

1. INTRODUCTION

M2-52 (PN G 103.7+00.4) is a bipolar planetary nebula classified by Manchado et al. (1996) as a **Br-type** (bipolar with a ring) nebula. The nebula shows faint extensions beyond a central ring. According to Manchado et al. (1996) its dimensions are: total diameter of $60''$ and central ring diameter of $23''$. Acker et al. (1992) have reported a

flux at $\text{H}\beta$, not corrected for reddening, $F(\text{H}\beta) = 5.01 \times 10^{-13} \text{ erg cm}^{-2} \text{ s}^{-1}$; this flux was computed by assuming a diameter of $14''$ for the whole nebula.

As with other Br-type planetary nebulae (PNe) studied to date, M2-52 has been found to have an important amount of molecular material in the ring. Guerrero et al. (2000) have found a large amount of H_2 with a total flux of $F(\text{H}_2) = 1.98 \times 10^{-12} \text{ erg cm}^{-2} \text{ s}^{-1}$. The same authors established that, in comparison with the $\text{Br}\gamma$ emission,

¹Based on data collected at the Observatorio Astronómico Nacional in San Pedro Mártir, B. C., México.

M2-52 appears as a H_2 -dominated PN, with a ratio $F(H_2)/F(Br\gamma) = 8.6$. In addition, Zhang et al. (2000) have reported the detection of molecular CO(1-0) in this object, with an intensity corresponding to a molecular mass of about $0.085M_\odot$ if they assume a distance of 4.2 kpc. Guerrero et al. (2000) and Zhang, Sun, & Ping (2000) found that the molecular material is located in the ring and concentrated in two bright knots separated (from peak to peak) by about $7''$. Zhang et al. derived a radial velocity of -63.2 km s^{-1} for this object.

An expansion velocity of 7.5 km s^{-1} has been measured by Sabbadin, Ortolani, & Bianchini (1985), by fitting two Gaussian components to the [O III] 5007 line, which appears single and broad.

Condon & Kaplan (1998) presented radio observations at 1.4 GHz of a great number of Galactic planetary nebulae. For M2-52 they have reported a flux $S_\nu = 15.4 \pm 0.6 \text{ mJy}$, which they combined with the total flux at $H\beta$ to compute the logarithmic reddening correction at $H\beta$, obtaining a value of $c(H\beta) = 1.0$.

From optical spectroscopy, Kaler et al. (1996) found that M2-52 can be classified as a Peimbert's Type I planetary nebula. Type I PNe characteristically show large He and N enrichment and presumably they evolve from the most massive PN progenitor stars. These objects are potentially an important source of He and N enrichment in the interstellar medium. A substantial fraction of Type I PNe shows bipolar morphology and a noteworthy filamentary structure (Peimbert 1978; Peimbert 1985 and references therein).

In this work we present high-resolution spectrophotometric data for the central zone of M2-52, demonstrating that it is an extreme Type I planetary nebula, comparable to the outstanding NGC 2440 and NGC 2818. In § 2, we describe the observations and data reduction. The analysis of kinematics and photometric data is discussed in § 3, and in § 4 we summarise our results.

2. OBSERVATIONS AND DATA REDUCTION

Two high-resolution echelle spectra with exposure times of 10 min and 20 min, respectively, were obtained on 2000 November 2, with the 2.1-m telescope and the Thomson TH7398M CCD (2048×2048 pixels of $14 \times 14 \mu\text{m}$), at the Observatorio Astronómico Nacional (OAN), San Pedro Mártir, B. C., México. Slit dimensions were $4''$ along the dispersion and $13.3''$ along the spatial coordinate. The slit was E-W oriented and the spectral range covered was from 3300 to 7300 Å, with a spectral resolution between 0.1 and 0.2 Å. Th-Ar comparison lamps were

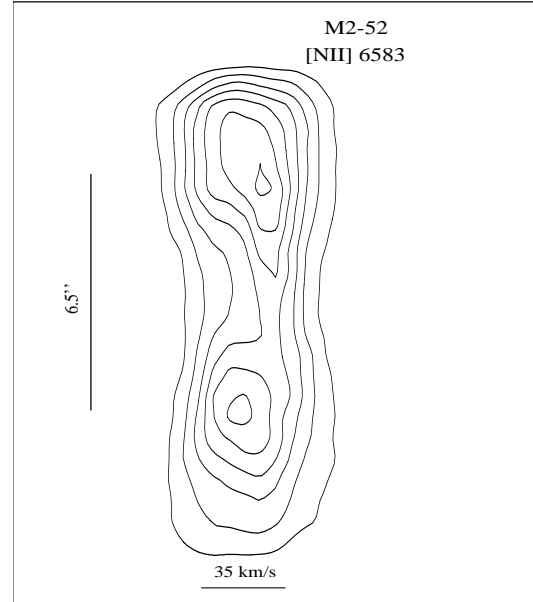


Fig. 1. Contour diagram of the [N II] 6583 emission line in the bi-dimensional spectrum. The spatial direction is along the y axis. The two knots detected are oriented E-W (East is up), and separated by $6.5''$. The stellar continuum should be located between the knots, but the star is too faint to be detected in our echelle spectrum. The emission is filling the slit of $13.3''$ length. The FWHM of the [N II] line is 0.95 \AA , equivalent to a velocity range of 35 km s^{-1} .

used for wavelength calibration and three standard stars from the list of Hamuy et al. (1992) were observed for flux calibration.

Due to the large extent of M2-52, our slit included only the central zone and part of the bright ring around the central star. The bipolar nature of M2-52 is evident in our bi-dimensional spectra. Figure 1 shows the structure of the [N II] 6583 emission line. The emission is extended, filling the slit along the spatial axis, and two bright knots are clearly detected, separated by 6.5 arcsec. The stellar continuum emission should be located in the middle, between the knots, but the star is too faint to be detected in our high resolution spectrum. All the nebular lines present in our spectrum show a similar structure, except He II 4686 for which the knots appear less defined. That is, the He II emission is more concentrated towards the central zone nearer the central star. The knotty structure we have detected agrees well with the morphology presented by Guerrero et al. (2000, see their Fig. 1b). The knots observed in [N II] almost coincide with the bright knots in H_2 found by them. Both emissions arise from the ring of the nebula.

TABLE 1
OBSERVED AND DEREDDENED FLUXES OF M2-52, RELATIVE TO H β

Ion	λ	f_λ	Center Zone (4'' \times 3'')		East Knot (4'' \times 3'')		All (4'' \times 13'')	
			$F_\lambda/F(\text{H}\beta)$	$I_\lambda/I(\text{H}\beta)$	$F_\lambda/F(\text{H}\beta)$	$I_\lambda/I(\text{H}\beta)$	$F_\lambda/F(\text{H}\beta)$	$I_\lambda/I(\text{H}\beta)$
[O II]	3726	0.256	0.42:	0.85:	0.56	1.36	0.50	1.14
[O II]	3729	0.255	0.40:	0.81:	0.54	1.30	0.55:	1.25:
[Ne III]	3869	0.223	0.90	1.67	1.02	2.16	0.93	1.91
[Ne III]	3967	0.203	0.32	0.65
[S II]	4069	0.178	0.06:	0.11:
C II	4267	0.141	< 0.01	< 0.02
H γ	4340	0.125	0.34	0.47	0.30	0.46	0.32	0.46
[O III]	4363	0.124	0.13	0.18	0.15	0.24	0.15	0.22
He II	4686	0.042	0.83	0.93	0.75	0.87	0.72	0.83
[Ar IV]	4711	0.039	0.11:	0.12:	0.12	0.13	0.09	0.10
[Ne IV]	4725	0.035	0.02:	0.02:	0.01:	0.02:
[Ar IV]	4741	0.031	0.09:	0.10:	0.10	0.11	0.08	0.08
[O III]	4959	0.023	4.30	4.03	4.50	4.16	4.04	3.75
[O III]	5007	-0.033	12.90	11.77	14.10	12.58	13.5	12.13
[N I]	5200	-0.073	0.11:	0.09:	0.16:	0.12:
He II	5411	-0.118	0.12	0.08	0.12	0.09	0.11	0.07
[N II]	5755	-0.185	0.22	0.13	0.40	0.21	0.34	0.19
He I	5876	-0.208	0.18	0.10	0.25	0.12	0.23	0.12
[O I]	6300	-0.284	0.14	0.06	0.25	0.09	0.36	0.14
[S III]	6312	-0.286	0.16	0.07	0.21	0.08	0.18	0.06
H α	6563	-0.330	7.10	2.83	8.75	2.80	8.14	2.81
[N II]	6583	-0.335	15.14	6.00	27.92	8.78	23.90	8.13
[S II]	6717	-0.343	0.92	0.36	1.62	0.50	1.61	0.53
[S II]	6731	-0.344	0.92	0.35	1.69	0.52	1.61	0.53
[Ar V]	7006	-0.375	0.19	0.07	0.14	0.05	0.14	0.04
[Ar III]	7136	-0.390	1.07	0.36	1.17	0.26	1.15	0.37
$c(\text{H}\beta)$			1.2 ± 0.2		1.5 ± 0.2		1.4 ± 0.2	
$\log F(\text{H}\beta)$ (erg cm $^{-2}$ s $^{-1}$)			-14.00		-13.82		-13.25	

Our bi-dimensional echelle spectra were bias-subtracted and flat-fielded using IRAF standard procedures.² Then we proceeded to extract spectral data of three different zones: The central zone between the knots was extracted with an aperture of $4 \times 3''$ (it would correspond to the zone nearest to the central star); the emission from the East knot was extracted with an aperture of also $4 \times 3''$ and, finally, we extracted almost all the nebular emission in our slit with an aperture of $4 \times 13''$. Extracted

spectra were wavelength- and flux-calibrated. Our final spectra are an average of the two observations.

In Table 1 we present the observed fluxes, F_λ , and the dereddened fluxes, I_λ , relative to H β , for the most important lines detected in the three zones. The dereddened fluxes were derived from the observed fluxes employing a logarithmic reddening correction at H β , $c(\text{H}\beta)$, as derived for each zone, from the Balmer decrement by considering case B recombination theory (Hummer & Storey 1987). We used the reddening law, f_λ , given by Seaton (1979), which is listed in column 3 of Table 1. The values for $c(\text{H}\beta)$

²IRAF is distributed by NOAO, which is operated by AURA, Inc., under contract with the NSF.

TABLE 2
PHYSICAL CONDITIONS AND CHEMICAL COMPOSITION

	Center Zone	East Knot	All
$T[\text{O III}]$	14800 ± 1200	14600 ± 1100	14600 ± 1000
$T[\text{N II}]$	12300 ± 1200	12800 ± 1200	12500 ± 1000
$N[\text{S II}]$	600 ± 400	800 ± 400	700 ± 400
$N[\text{Ar IV}]$	1700 ± 800	1200 ± 800	800 ± 600
$N[\text{O II}]$	610:	700:	500:
$\text{He}^+(5876)$	7.20×10^{-2}	8.55×10^{-2}	8.40×10^{-2}
$\text{He}^{++}(4686)$	9.10×10^{-2}	8.49×10^{-2}	8.06×10^{-2}
$\text{N}^+(6583)$	5.87×10^{-5}	8.26×10^{-5}	7.73×10^{-5}
$\text{O}^+(3727)$	2.47×10^{-5}	3.69×10^{-5}	3.34×10^{-5}
$\text{O}^{++}(5007)$	1.27×10^{-4}	1.42×10^{-4}	1.36×10^{-4}
$\text{Ne}^{++}(3869)$	4.24×10^{-5}	5.78×10^{-5}	5.05×10^{-5}
$\text{Ne}^{+3}(4725)$	2.56×10^{-5}	2.79×10^{-5}	2.19×10^{-5}
$\text{S}^+(6730)$	8.59×10^{-7}	1.23×10^{-6}	1.27×10^{-6}
$\text{S}^{++}(6312)$	4.16×10^{-6}	4.70×10^{-6}	3.85×10^{-6}
$\text{Ar}^{++}(7136)$	1.48×10^{-6}	1.09×10^{-6}	1.54×10^{-6}
$\text{Ar}^{+3}(4740)$	6.68×10^{-7}	7.33×10^{-7}	5.47×10^{-7}
$\text{Ar}^{+4}(7006)$	4.72×10^{-7}	3.29×10^{-7}	2.72×10^{-7}
He/H	0.163 ± 0.010	0.170 ± 0.010	0.165 ± 0.010
O/H	$(2.6 \pm 0.5) \times 10^{-4}$	$(2.8 \pm 0.5) \times 10^{-4}$	$(2.6 \pm 0.5) \times 10^{-4}$
N/O (N^+/O^+)	2.4 ± 0.3	2.2 ± 0.3	2.3 ± 0.3
Ne/O ($\text{Ne}^{++}/\text{O}^{++}$)	0.33 ± 0.15	0.41 ± 0.15	0.37 ± 0.15
S/H ($\text{S}^+ + \text{S}^{++}$)	$> 5.0 \times 10^{-6}$	$> 5.9 \times 10^{-6}$	$> 5.1 \times 10^{-6}$
Ar/H ($\text{Ar}^{++} + \text{Ar}^{+3} + \text{Ar}^{+4}$)	$(2.7 \pm 0.5) \times 10^{-6}$	$(2.2 \pm 0.4) \times 10^{-6}$	$(2.4 \pm 0.5) \times 10^{-6}$

are given at the bottom of Table 1. In the three regions we found similar reddening coefficients (within uncertainties), though it is interesting to notice that the knot presents a slightly larger reddening, probably due to the molecular material located near this region.

As expected from the ionization structure of photoionized nebulae, the line intensities of low ionization species appear to be larger in the knot, far from the central star, than in the central zone.

Uncertainties in the line ratios were determined by comparing the measurements of our two spectra. In a general way, the uncertainties for lines with $F_\lambda/F(\text{H}\beta) \geq 0.2$ are better than 10% and improve with the line flux (for instance, the uncertainties for $[\text{O III}] 5007$ are about 3%). The exceptions are $[\text{O II}] 3726$ and 3729 for which uncertainties of about 20% are found. This is because the large reddening affecting M2-52 weakens the UV lines. Lines with $0.2 > F_\lambda/F(\text{H}\beta) > 0.05$ (such as the important

$[\text{O III}] 4363$ and $[\text{N II}] 5755$), have uncertainties of about 20%, and the uncertainties are larger for lines marked with a colon. The fluxes at $\text{H}\beta$, as measured with the different extraction apertures, are given at the end of Table 1.

Plasma diagnostics were calculated from the emission line ratios in a standard way, using the same atomic data as listed in Stasińska & Leitherer (1996).

Electron densities were derived from $[\text{O II}] 3726/3729$, $[\text{S II}] 6717/6731$, and $[\text{Ar IV}] 4711/4740$ line ratios, electron temperatures were measured from $[\text{O III}] 4363/5007$ and $[\text{N II}] 5755/6583$ ratios. The density used for deriving the electron temperatures was that deduced from $[\text{S II}] 6717/6731$, which is more reliable and equal, within uncertainties, to the density obtained from the $[\text{Ar IV}]$ and $[\text{O II}]$ lines.

The derived electron temperatures and densities are listed in Table 2, together with the errors based on the uncertainties of the line ratios described above. We do not find any systematic difference in

the temperatures of the different regions. Temperatures and densities are equal in the central zone and in the knot, within uncertainties, although the knot could be slightly denser.

Ionic abundances were then obtained for the three regions, using $T[\text{O III}]$ for the high ionization species and $T[\text{N II}]$ for the low ionization ones. Electron densities derived from $[\text{S II}]$ 6717/6731 ratios were always used. The results are presented in Table 2, where we also indicate which emission line has been employed to derive the ionic abundance. No temperature fluctuations were considered in deriving the ionic abundances; therefore, they should be considered as lower limits of the true chemical abundances (See Peimbert et al. 1995 for a discussion of the effects of temperature fluctuations on chemical abundance determinations). However, due to the low density in the nebula, we do not expect very large deviations of the derived chemical abundances.

Elemental abundance ratios were computed from the ionic abundance ratios using the ionization correction factors of Kingsburgh & Barlow (1994). The abundance ratios He/H, O/H, N/O, Ne/O, S/H, and Ar/H are given at the bottom of Table 2. The value for S/H is the sum $(\text{S}^+ + \text{S}^{++})/\text{H}^+$, while the value for Ar/H is the sum of the Ar^{++} , Ar^{+3} , and Ar^{+4} abundances; therefore, only Ar/H can be considered a reliable value. The error bars that are listed for O, N, Ne, and Ar abundances take into account the uncertainties propagated from the uncertainties in the physical conditions (electron temperature and density).

3. DATA ANALYSIS AND DISCUSSION

3.1. Kinematics

Our echelle spectra have a resolution better than 10 km s^{-1} on average, which is good enough to derive the radial and expansion velocities of the nebula. We find that the heliocentric radial velocity, as measured from all the available lines, is $-73 \pm 7 \text{ km s}^{-1}$, in good agreement with the values presented in previous works.

Analyzing the structure of $[\text{N II}]$ 6583 line shown in Fig. 1, it is found that the knots situated on each side of the central star do not show a significant difference in velocity (they appear well aligned along the y axis), and the same is found for the other ions. If the knots belong to the ring which is forming the “waist” of the bipolar structure, as suggested by Guerrero et al. (2000), such a ring does not present important expansion nor rotation.

We have analyzed the line profiles of the ions present in the gas for the central zone spectra. All

TABLE 3
EXPANSION VELOCITIES

Ion	$2v_{\text{exp}}$ (km s^{-1})
He II (4686, 5411)	45 ± 4
He I (5876)	38 ± 7
[O III] (5007, 4959)	39 ± 4
H I ($\text{H}\alpha$, $\text{H}\beta$, $\text{H}\gamma$)	45 ± 4
[N II] (5755, 6548, 6583)	36 ± 3
[S II] (6717, 6731)	36 ± 4

the lines appear single (not split) but well resolved, and we have measured the FWHM of each line, proceeding then to subtract the instrumental width.

It is usual in the literature to interpret the separation of double-peak lines (or the FWHM of single lines) as an expansion velocity of the nebular shell, although a certain amount of turbulence and other parameters, such as density and thermal structures, could also be contributing to the line shapes and widths. Gesicki, Acker, & Szczerba (1996) and Neiner et al. (2000) have demonstrated that for the case of PNe ionized by non-[WC] central stars (as is the case for M2-52), the turbulent velocity field is negligible and the expansion velocity increases from high to low ionization species.

We have determined the expansion velocities of the different ions present in M2-52 from the FWHM of their lines. These values are listed in Table 3. The uncertainties in this table have been computed by taking into account the measurements, in both spectra, of the available emission lines for each ion.

Within uncertainties, all the ions present similar expansion velocities, and an average $v_{\text{exp}} \sim 20 \pm 2 \text{ km s}^{-1}$ could be adopted for the nebula. Nevertheless, it is notable that low ionization species such as N^+ and S^+ show systematically lower expansion velocities ($18 \pm 3 \text{ km s}^{-1}$) than He^{++} and H^+ , for which $v_{\text{exp}} \sim 22 \pm 4 \text{ km s}^{-1}$. Also, O^{++} and He^+ show lower expansion than He^{++} and H^+ . This behavior is opposite to the one found by Gesicki et al. (1996) and Neiner et al. (2000) and should be verified with better resolution spectroscopic data. If real, it could be indicating that the less ionized zones of the nebula (where N^+ and S^+ are located) are being decelerated by the torus of molecular material around the central star. It would be interesting to verify if such a behavior is found in other Br-type PNe.

Our value of v_{exp} for M2-52 is larger than the one reported by Sabbadin et al. (1985). This is due to

the different measuring methods employed. We have fitted single Gaussians to the line profiles because, as we said before, the lines appear single and one Gaussian distribution is an adequate fit. Sabbadin et al. (1985) have adjusted two Gaussians to the single profile, taking $2v_{\text{exp}}$ as equal to the difference in velocity of the two maxima of both Gaussians. Their procedure produces a lower v_{exp} .

3.2. Ionic and Total Abundances

M2-52 shows an emission-line pattern similar to those of other Type I PNe, in the sense that high and low ionization lines are present. We have detected lines of Ar^{+3} as well as of O^0 in the central zone and also in the knot, although the knot presents a lower excitation and the lines of low ionization species are enhanced in this zone. This difference in excitation is due to the normal ionization structure of a nebula photoionized by a hot central star. The highly ionized gas is closer to the star.

The ionization degree in M2-52 is very high, as deduced by the large fraction of twice ionized He ($\text{He}^{++}/\text{He} = 0.50$ in the knot and 0.56 in the center). This indicates a high effective temperature for the central star (certainly hotter than 80,000 K). Unfortunately the central star is faint and in our high-resolution spectra we have not detected the stellar emission, thus no Zanstra temperature could be derived.

The elemental abundances of M2-52, presented in Table 2, are equal, within uncertainties, in the central zone and in the knot and, in the following, we will adopt the values obtained for the whole nebula for our analysis. As shown in Table 2, M2-52 is a very He- and N-rich nebula. The high He/H ratio of 0.165 is one of the largest reported for Type I PNe and it is only comparable to the values of NGC 2818 (Peimbert & Torres-Peimbert 1987) and He 2-111, the extreme Type I PN reported by Kingsburgh & Barlow (1994). Also the N/O ratio of 2.3 is one of the largest reported, and it is similar to the large N/O value of NGC 2440, considered as the prototype of Peimbert's Type I PNe. For the latter nebula, Hyung & Aller (1998) have computed a N/O ratio of 2.16, which they consider could be an artifact produced by "abnormally" strengthened [N II] lines in the blobs of NGC 2440. Other similarities between M2-52, NGC 2818, and NGC 2440 are remarkable; for instance, the electron temperatures are very similar in these objects (Peimbert et al. 1995), indicating similar heating and cooling processes. Also the morphology of M2-52 is very similar to that of NGC 2818 and NGC 2440.

Comparing our values for M2-52 with those obtained by Kaler et al. (1996), we find that our line ratios and physical conditions are similar to theirs, except for the logarithmic reddening correction $c(\text{H}\beta)$ for which they derive a value of 1.6, larger than our 1.2 ± 0.2 for the center and 1.4 ± 0.2 for the whole nebula. This discrepancy is the reason why Kaler et al. have found a lower N/O ratio, due to the larger extinction correction applied to their [O II] 3727 doublet. A value for $c(\text{H}\beta)$ can be estimated from the observed flux of $\text{Br}\gamma$ ($2.3 \times 10^{-13} \text{ erg cm}^{-2} \text{ s}^{-1}$) given by Guerrero et al. (2000), relative to the total $\text{H}\beta$ flux given by Acker et al. (1992). By adopting a theoretical $\text{Br}\gamma/\text{H}\beta$ ratio of 0.028 (Osterbrock 1989) and a reddening correction factor for $\text{Br}\gamma$, $f_{\lambda} = -0.901$ (Cardelli, Clayton, & Mathis 1989) we have deduced $c(\text{H}\beta) = 1.36$, in very good agreement with our value from the Balmer decrement. Also our value of $c(\text{H}\beta)$ is similar to the reddening reported by Condon & Kaplan (1998) from radio observations of M2-52. Therefore, we have confidence in our results.

As in other Type I PNe, the extreme He- and N-enrichment in M2-52 indicates that the central star experienced envelope-burning conversion to nitrogen of primary carbon extracted during the third dredge-up event. Unfortunately we were not able to determine the carbon abundance of M2-52, due to the weakness of the C II 4267 emission line, for which only an upper limit is given. It is possible that carbon is also enhanced in M2-52, as it is in NGC 2440 (Hyung & Aller 1998), due to the notable similarities between physical conditions and chemical composition in both nebulae.

4. CONCLUSIONS

The Br-type nebula M2-52 appears to be a high-excitation Type I PN with a rich spectrum including high and low excitation lines. From high resolution spectrophotometry of the central zone, we have found that the ionized shell shows an expansion velocity of about $20 \pm 2 \text{ km s}^{-1}$. The low ionization species, however, seem to have slightly lower expansion velocities than the high ionization ones. This could indicate that the ring of molecular material detected around the central star is decelerating the expansion of the external zones of the ionized gas. Better resolution spectroscopy is required to confirm this result.

The physical conditions in the ionized gas are: $T[\text{O III}] = 14600 \pm 1000 \text{ K}$, $T[\text{N II}] = 12500 \pm 1000 \text{ K}$, electron density $\sim 800 \text{ cm}^{-3}$, and the chemical composition is: $\text{He}/\text{H} = 0.165 \pm 0.010$, $\text{O}/\text{H} = (2.6 \pm 0.5) \times 10^{-4}$, $\text{N}/\text{O} = 2.3 \pm 0.3$,

$\text{Ne/O} = 0.37 \pm 0.15$, $\text{Ar/O} = (9.2 \pm 2.0) \times 10^{-3}$, and $\text{S/O} > 2.0 \times 10^{-3}$.

Our oxygen abundance for M2-52 is a relatively low value when compared with the O/H abundances derived for other Type I PNe by Peimbert et al. (1995). This is understandable when we consider that Peimbert et al.'s values include the effects of temperature fluctuations. On the other hand, the abundance ratios relative to oxygen are not as affected by this phenomenon because the ratios are not strongly temperature dependent; therefore, the N/O, Ne/O, and Ar/O ratios are reliable values. The large He/H and N/O ratios clearly establish that M2-52 is a Peimbert Type I PN, presenting one of the largest known He and N enrichments, similar to the values for NGC 2440 and NGC 2818. Neon and argon abundances in M2-52, relative to oxygen, are in very good agreement with the bulk of Type I PNe (Kingsburgh & Barlow 1994; Peimbert et al. 1995).

This work received partial support from DGAPA/UNAM (grant IN100799) and CONACyT (grant 35594-E). S.M. acknowledges scholarship from DGEP/UNAM and CONACyT.

REFERENCES

- Acker, A., Marcout, J., Oksenbein, F., Stenholm, B., & Tylenda, R. 1992, *The Strasbourg-ESO Catalogue of Galactic Planetary Nebulae*
- Cardelli, J. A., Clayton, G. C., & Mathis, J. S. 1989, *ApJ*, 345, 245
- Condon, J. J., & Kaplan, D. L. 1998, *ApJS*, 117, 361
- Gesicki, K., Acker, A., & Szczerba, R. 1996, *A&A*, 309, 907
- Guerrero, M. A., Villaver, E., Manchado, A., García-Lario, P., & Prada, F. 2000, *ApJS*, 127, 125
- Hamuy, M., Walker A. R., Suntzeff N. B., et al. 1992, *PASP*, 104, 533
- Hummer, D. G., & Storey, P. J. 1987, *MNRAS*, 224, 609
- Hyung, S., & Aller, L. H. 1998, *PASP*, 110, 466
- Kaler, J. A., Kwitter, K. B., Shaw, R. A., & Browning, L. 1996, *PASP*, 108, 980
- Kingsburgh, R. L., & Barlow, M. J. 1994, *MNRAS*, 271, 257
- Manchado, A., Guerrero, M. A., Stanghellini, L., & Serra-Ricart, M. 1996, *The IAC Morphological Catalog of Northern Galactic Planetary Nebulae (Laguna: IAC)*
- Neiner, C., Acker, A., Gesicki, K., & Szczerba, R. 2000, *A&A*, 358, 321
- Osterbrock, D. 1989, *Astrophysics of Gaseous Nebulae and Active Galactic Nuclei (Mill Valley: University Science Books)*
- Peimbert, M. 1978, in *IAU Symp. No. 76, Planetary Nebulae: Observations and Theory*, ed. Y. Terzian (Dordrecht: Reidel), 215
- Peimbert, M. 1985, *RevMexAA*, 10, 125
- Peimbert, M., & Torres-Peimbert, S. 1987, *RevMexAA*, 14, 540
- Peimbert, M., Luridiana, V., & Torres-Peimbert, S. 1995, *RevMexAA*, 31, 147
- Sabbadin, F., Ortolani, S., & Bianchini, A. 1985, *MNRAS*, 213, 563
- Seaton, M. 1979, *MNRAS*, 185, 57
- Stasińska, G., & Leitherer, C. 1996, *ApJS*, 107, 661
- Zhang, H.-Y., Sun, J., & Ping, J.-S. 2000, *Acta Astronomica Sinica*, 41, 23